06

Stable sols of carboxylated diamond nanoparticles in dimethyl sulfoxide

© D.E. Martyanov, A.T. Dideikin, A.D. Trofimuk, A.Ya. Vul'

Ioffe Institute,
194021 St. Petersburg, Russia
e-mail: molibdenchik@mail.ioffe.ru

Received October 29, 2024
Revised October 29, 2024
Accepted October 29, 2024

Stable sols of diamond nanoparticles produced by detonation synthesis with negative electrokinetic potential in dimethyl sulfoxide, one of the most common non-aqueous solvents widely used in organic synthesis and medicine, were obtained for the first time. Sol stability is achieved by steric stabilization of the surface of diamond nanoparticles due to a cationic surfactant, cetyltrimethylammonium bromide, which binds to the carboxyl groups of diamond nanoparticles. The obtained stable sols can be used for subsequent chemical modification of the surface of diamond nanoparticles.

Keywords: Diamond nanoparticles, detonation synthesis, dimethyl sulfoxide, sols, stability of colloidal systems, surfactants.

DOI: 10.61011/TP.2025.02.60837.369-24

Introduction

Unique set of physical and chemical properties of diamond that is kept during the transition to nanoscale particles — biocompatibility, chemical inertness with respect to most aggressive media, record-breaking hardness and thermal conductivity — defines the variety of applications of nanoscale diamond particles, so-called nanodiamonds [1].

Scope of application of nanodiamonds fabricated by the detonation synthesis method — detonation nanodiamonds (DND) — hasn't been completely outlined yet. Publications of past years [2–5] show that DND may be used to create various composite materials, including polymer materials, metal catalyst carriers, effective nucleation centers during CVD diamond film growth, as antifrictional materials, for single-photon radiation sources based on nitrogen-vacancy color centers. However, the main focus is made on biomedical applications of DND, including targeted delivery of drugs and contrast agents for magnetic resonance imaging [5–7].

For some applications, it is critical to produce stable sols of diamond nanoparticles [8].

This problem is solved for hydrosols. DND agglomerate disaggregation to 4−5 nm primary particles was first achieved by E. Ōsawa et al. by mechanical milling of DND agglomerates with ZrO_2 microparticles [9]. Later, methods of reductive [10] and oxidative [11] annealing in hydrogen and air, respectively, were proposed, which make it possible to obtain stable hydrosols of primary DND particles without any mechanical treatment.

Production of stable colloidal solutions in non-aqueous media will significantly facilitate the development of DND applications [8,12]. So, for example, the most promising methods to produce polymer composites are production through polymer solution [13,14] and *in situ* monomer polymerization in the presence of nanoparticles [4,15,16]. As polymers and monomers are often poorly water soluble, production of stable DND sols in non-aqueous media is an important task. Utilization of DND colloidal solutions in organic solvents is also important for creating lubricants [17], coolants and heat-transfer liquids [18] as well as for solution of various biomedical tasks [12,19].

However, for non-aqueous solvents, the problem of producing stable diamond nanoparticle sols is solved only partially. Stable colloidal DND solutions in ethyleneglycol, glycerol, N-methylpyrrolidone, dimethylformamide (DMFA), kerosene and synthetic polyalphaolefin oil have been obtained to date without any preliminary surface treatment, only due to the presence of functional groups with certain composition, mainly -COOH carboxyl groups [8,20], on the surface. It was shown in [21] that carboxylated DND's also form stable colloidal solutions in methanol.

The use of surfactants makes it possible to obtain stable colloidal solutions of oxidized (with negative electrokinetic potential) DND particles in toluene and chloroform [22], as well as in tetrahydrofuran (THF), methyl ethyl ketone and acetone [23]. Stabilization was achieved by means of surface modification of oxidized particles by amine-containing surfactants (octadecylamine and oleylamine) that form complexes during interaction with ionized carboxyl groups on the DND surface.

One of the most common non-aqueous solvents is dimethyl sulfoxide (DMSO). Unique dissolving ability and minimal toxicity among polar aprotic solvents define its wide use in organic synthesis [24–28] and medicine [24,29,30]. It is commonly known that DMSO is the best, compared with water, solvent for such substances as proteins and enzymes. Therefore, solutions of DND in DMSO are expected to have a higher reactivity in biological media. As dimethyl sulfoxide is water-miscible in any proportions, DND particles suspended in DMSO

may be easily transferred into aqueous solutions. DMSO can also facilitate better cutaneous penetration of DND for administration of antivirals, steroids and antibiotics [31,32].

DMSO as a polar aprotic solvent also plays an important role in organic synthesis being one of the most preferable solvents in bimolecular nucleophilic substitution reactions (S_N2). DMSO molecule has a partially negative charge $\delta-$ on the oxygen atom, due to which DMSO solvates cations well. Furthermore, the electron-deficient region $\delta+$ is located in the center of the compound and is surrounded by lone electron pairs and methyl groups, thus making it sterically hard-to-reach for anions. This structural feature of DMSO (as well as of other polar aprotic solvents) defines its low anion solvation capability. Due to low anion solvation, dimethyl sulfoxide makes nucleophilic particles more reactive in S_N2 type reactions [25,26].

The authors of [33] consider that stable colloidal solutions of diamond nanoparticles in dimethyl sulfoxide may be suitable for applications such as diamond CVD-film growing, surface polishing and mechanochemical treatment as well as for processes involving the application and removal of photoresist. In addition, it was shown in the same work that the use of DMSO makes it possible to more efficiently and cheaply isolate particles with a positive electrokinetic potential of less than 50 nm in size from polydisperse DND samples than using water or other organic solvents. Review [12] reports that DMSO-based colloidal solutions may be also used to create polymer composites.

Thus, DND particle stabilization in DMSO will significantly broaden the scope of application of diamond nanoparticles produced by detonation synthesis. However, this task cannot be considered as completely solved [8]. Indeed, as far as we know, the production of stable DMSO-based sols has been reported only using diamond nanoparticles produced by detonation synthesis with a positive electrokinetic potential (ξ potential) [33,34].

At the same time, the nature and properties of nanodiamonds with positive ξ-potential are currently the subject of discussions and are poorly understood [35]. In addition, the starting point for almost any surface modification is the use of already well-studied diamond nanoparticles with a negative ξ-potential, primarily due to the presence of synthetically universal carboxyl groups on the surface. Therefore, obtaining stable sols of diamond nanoparticles with negative electrokinetic potential in dimethyl sulfoxide is an unsolved and urgent task.

Note that oxidized DND samples were studied in [33]. The authors emphasized low stability of DND colloids in DMSO. In [20], stable DND sols in DMSO were obtained only when the oxidized surface of particles was reduced by lithium aluminum hydride.

Paper [36] shows experimentally that DND oxidized at 400°C and purified with chloric acid are dispersed and remain stable during 24 h in solvents with high polarity and corresponding Hansen parameters for hydrogen bonds such as DMSO, dimethylacetamide and DMFA. Nevertheless, it is remarkable that in the infrared (IR) spectra of the DND, the peak belonging to the carboxyl groups (1720 cm^{-1}) has an extremely low intensity, while there are also positions 2920 and 2850 cm^{-1} corresponding to vibrations of the C−H bonds. The latter is obviously indicative of the fact that the surface of DND used in the work is heterogeneous and not fully oxidized. This is also confirmed by positive ξ-potential of DND in hydrosols. In addition, the surface of the samples contains amino and nitro groups, which complicates interpretation of the stability mechanism of suspensions obtained in the work.

Thus, to date, stable DND sols with an oxidized surface have not been obtained in one of the most important polar aprotic solvents of medium (according to the Fialkov classification [37,38]) polarity, widely used in medicine and organic synthesis, dimethyl sulfoxide. Solving this problem will significantly develop the fields of application of both DND and DMSO, and will contribute to a better understanding of the properties of detonation nanodiamonds at a fundamental level. The objective of this study was to solve this problem.

1. Samples and research methods

1.1. Samples

Hydrosol of diamond nanoparticles produced by detonation synthesis made from industrial DND powders using a technique developed by the Laboratory of Physics for Cluster Structures of Ioffe Institute [11] was used as the feedstock for the study. According to the dynamic light scattering (DLS) method, mean size of particles in the hydrosol was equal to 4−5 nm.

Cetyltrimethylammonium bromide (n-$C_{16}H_{33}N(CH_3)_3Br$, CTAB) (99+%, Acros Organics BV, Catalog No. 227160100) was used as a surfactant.

Dimethylsulfoxide ($CH_3S(O)CH_3$, DMSO) (chemically pure, STP TU KOMP 2-451-2011) was used to prepare organosols. ASTM type 2 deionized water (with a resistivity of 5−10 MΩ·cm) was used for the study.

1.2. Research methods

The elemental composition of the DND samples was determined by the electron microprobe (EMP) using the TESCAN VEGA 3 SBH scanning electron microscope with the AdvancedAztecEnergy element composition determination system on the basis of the X-act semiconductor energy-dispersive detector made by Oxford Instruments NanoAnalysis Ltd. (UK).

IR spectroscopy was used to examine the composition of surface functional groups of the DND samples and the spectrum of CTAB inoculated on the surface. Lumeks (Saint Petersburg, Russia) Infralum FT-08 Fourier transform IR spectrometer with a diffuse reflection module was used for the experiments. Spectra were plotted in the Kubelka-Munk coordinates.

Ultraviolet and visible (UV-Vis) absorption spectra were recorded using the single-beam UNICO 2800 UV/VIS

spectrophotometer (USA) in the scanning mode in the wavelength range from 190 nm to 1100 nm. Photometric range of absorbance was 0.3−2.8. 3 ml of studied liquids were placed into quartz cells with sample thickness equal to 10 mm. Identical cells filled with pure solvent (deionized water, DMSO) were used as reference samples for each spectrum recording of real and colloidal solutions.

Also, to quantify the contribution of scattering to the UV-visible signal of the DND−CTAB sol in DMSO, spectra were recorded on a two-beam UV−VIS−NIR-spectrophotometer UV-3600 from Shimadzu (Japan), equipped with an ISR-3100 for UV-3600 integrating sphere. Spectra were recorded in the scanning mode in the wavelength range from 220 nm to 1000 nm. Thickness of the sample was 10 mm. Reference sample recording conditions are identical, the reference sample was recorded simultaneously with the studied one. To estimate the scattering contribution, difference spectra were plotted by subtraction of absorption spectra recorded with the integrating sphere from spectra recorded without it.

Phase composition of the initial DND sample was studied by the X-ray powder diffraction and Raman spectroscopy (RS). X-ray diffraction patterns were recorded using the Rigaku Corporation (Japan) SmartLab 3 diffractometer (CuK_α-radiation) in the angle range $2\theta = 5 - 130^\circ$ at 0.01° intervals, with a rate of 1°/min and K_β-filter. Mean crystallite sizes were estimated using the Selyakov-Scherrer equation. RS spectra were recorded using the NT-MDT Ntegra Spectra multifunctional system (Russia). The excitation radiation wavelength was 532 nm.

Measurements of particle size distributions in sols of the studied samples were carried out by the DLS using the Litesizer 500 from Anton Paar GmbH (Austria). The intensity of the radiation scattered on the samples was detected using a photoelectron multiplier located at an angle of 175° to the source (the intensity of backscattering was detected).

Electrophoretic mobility of diamond nanoparticles in sols was measured using the Litesizer 500 instrument made by Anton Paar GmbH (Austria) by the electrophoretic light scattering (ELS) method. Electrokinetic potential calculations used the Smoluchowski model for hydrosols and the Hückel model for sols in DMSO.

The electron spin resonance (ESR) method was used to study the initial and modified DND samples. ESR spectra were recorded at room temperature with 0.1 mT amplitude modulation and 3 mW microwave radiation power. ESR spectra were recorded in X range using the ESR 70-03 XD/2 desktop spectrometer made by UP KBSTU BGU (Belarus).

2. Experiment

2.1. DND surface modification by CTAB surfactant

As mentioned above, stabilization by surfactants is one of the possible approaches to production of stable DND particle sols [8]. This approach was implemented in this work. Cetyltrimethylammonium bromide, one of the most widely used surfactants, was chosen as a stabilizing agent that, being a cationic surfactant, shall be potentially bonded with anionic groups (preferably COO^-) on the DND surface.

Nanodiamond surface modification by surfactant was performed from the following consideration. It is known that the maximum number of ionized groups on the surface of one 4−5 nm DND particle is not higher than 60−65. The maximum possible number of ionized groups is achieved only in a strong alkaline medium, there are fewer ionized groups in a neutral medium [39]. Therefore, the amount of CTAB in this study was taken from the ratio of 30 surfactant molecules per a DND particle 4.5 nm in diameter.

The first surface modification step included preparation of the CTAB aqueous solution, for which accurately weighed 0.054 g of CTAB was dissolved in 10 ml of deionized water. For better dissolution of CTAB, the system was exposed to 22 kHz ultrasound during 2 min. 0.500 g of DND powder was added to the prepared cetyltrimethylammonium bromide solution, then the prepared colloidal solution was again exposed to 22 kHz ultrasound during 20 min.

Then, excess surfactant was removed from the system by centrifugation (the SIGMA 6-16 centrifuge with the 12169 rotor). The rotation speed was 4000 RPM, cycle time was 15 min.

The degree of removal of non-reacted CTAB from the system was controlled using the UV-Vis spectroscopy — CTAB absorption band intensity in supernatant was examined after each centrifugation cycle, deionized water served as a baseline. With centrifugation, absorption band intensity of an individual CTAB in supernatant liquid was getting reduced. The system was considered as washed when the intensity at all wavelengths was close to the instrument detection limit.

Upon removal of the surfactant molecules that hadn't reacted with DND particles, the system was dried in air at 120 °C. The prepared powder was triturated in an agate mortar.

2.2. Stability assessment of dimethyl sulfoxide-based sols

The next step included preparation of initial and CTAB-modified sols of DND samples in dimethyl sulfoxide. Colloidal stability of the prepared organsols was studied by successive utilizing spectrophotometry, dynamic and electrophoretic light scattering methods.

Sols were obtained by dispersing 1.534 g (0.22 weight%) of the initial DND sample and 1.401 g (0.20 weight%) of CTAB-modified DND in 700 g of dimethyl sulfoxide. Dispergation was performed using four 3 min cycles of 22 kHz ultrasonic treatment with intervals of several minutes between the ultrasound cycles to avoid excessive heating of liquid.

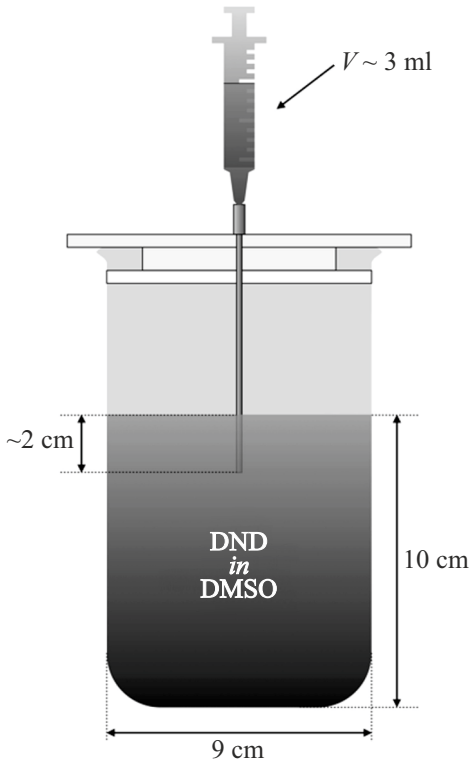

Figure 1. Setup for examining DND sedimentation in DMSO.

Dynamic and electrophoretic light scattering methods were used to record sizes and electrophoretic potentials, respectively, of particles in sols immediately after preparation.

Then, each sol sample was kept in a place protected from light and vibrations in a glass beaker (Figure 1) with a tight fluoropolymer cover (PTFE-4) with a special hole in which a stainless steel syringe needle was fixed. The needle was immersed at ~ 2 cm and left fixed in position throughout the experiment.

A cylindrical beaker ~ 9 cm in diameter was used, liquid height was ~ 10 cm. Such beaker dimensions imply small change in height during sampling, thus, making the measurement error negligible.

Then, the spectrophotometry was used to study the sedimentation stability of the prepared sols. This UV-Vis spectroscopy method was used to study the sedimentation of particles of the dispersed phase [40–42], in particular, diamond nanoparticles produced by detonation synthesis [20,36], in various liquids. Spectra were recorded during 120 h with discreteness that preserved the experiment accuracy during sampling.

3. Findings and discussion

3.1. Characterization of the initial samples

EMP of the initial DND sample (Table 1), as expected, shows high concentration of carbon ($> 90\%$) and oxygen ($\approx 10\%$), chlorine traces are also observed as a result of preliminary DND treatment with hydrochloric acid [43].

Mean diameter of DND particles in hydrosol is less than 10 nm as can be seen from the particle size distribution by the DLS (Figure 2, *a*). Distribution mode falls on ~ 4 nm particles.

The main feature of the Raman spectrum (Fig. 3, *a*) is a sharp asymmetric peak centered at $\approx 1328\,\mathrm{cm}^{-1}$ (diamond peak), indicating the crystalline structure of the diamond. The observed shift of the diamond band of the spectrum to the low-frequency region relative to the literary value of $1332\,\mathrm{cm}^{-1}$, characteristic of a bulk diamond, is a consequence of the phonon confinement effect and indicates the nanoscale of the object. Maximum at $1626\,\mathrm{cm}^{-1}$ is also typical of the DND RS spectra and its origin is most often associated with DND defects and attributed to stretching of the sp^2-hybridized amorphous carbon on the nanodiamond crystallite surfaces (this is a so-called G-line (Graphitic)) [1,44].

Diamond crystal structure of the studied sample is also confirmed by its X-ray diffraction pattern (Figure 3, *b*). Peaks correspond to the diamond crystal structure. The sample spectrum also shows a wide halo at $20 - 25°$ that corresponds to the amorphous sp^2-phase on the surface of diamond nanoparticles [45]. According to the assessment using the Selyakov-Scherrer equation, the mean crystallite size is about 4 nm.

Electron spin resonance spectrum (Figure 4, *a*) has a singlet peak typical of numerous defects contained in nanodiamond particles [46]. Line width $\Delta H_{pp} = 0.87$ mT, $g = 2.0019$. The absence of foreign peaks is indicative of the absence of metallic impurities and a proper degree of treatment of diamond nanoparticles.

The IR spectrum of the initial DND (Fig. 5, *a*) is characterized by the presence of a number of bands, the appearance of which is caused by vibrations in oxygen-

Table 1. Weight percentages of elements in DND samples, %

Sample	C	O	Cl	Total
Initial DND	91.45	8.43	0.12	100.00
DND modified by CTAB	90.58	9.31	0.11	100.00

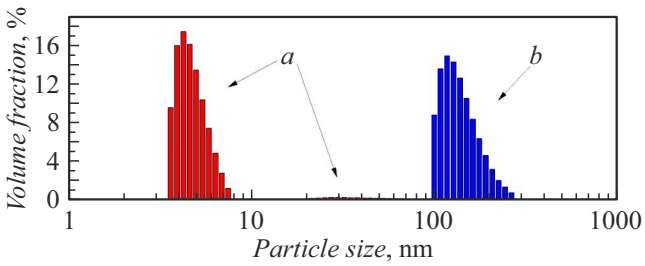

Figure 2. Size distribution of initial DND (*a*) and CTAB-modified DND particles (*b*) in hydrosol.

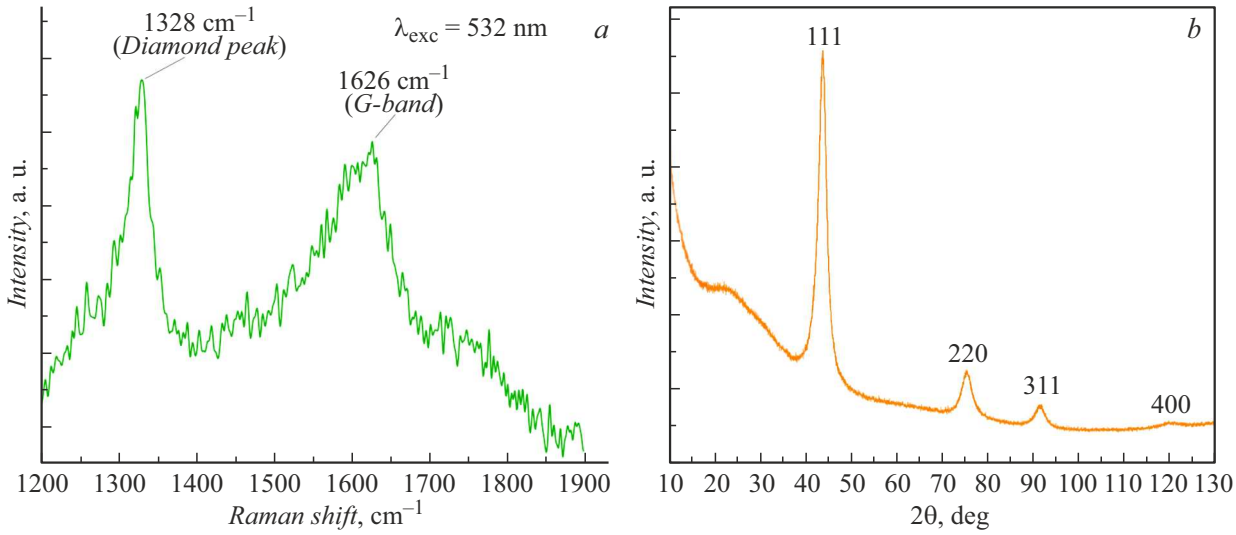

Figure 3. Raman spectrum (*a*) and X-ray diffraction pattern (*b*) of the initial DND sample.

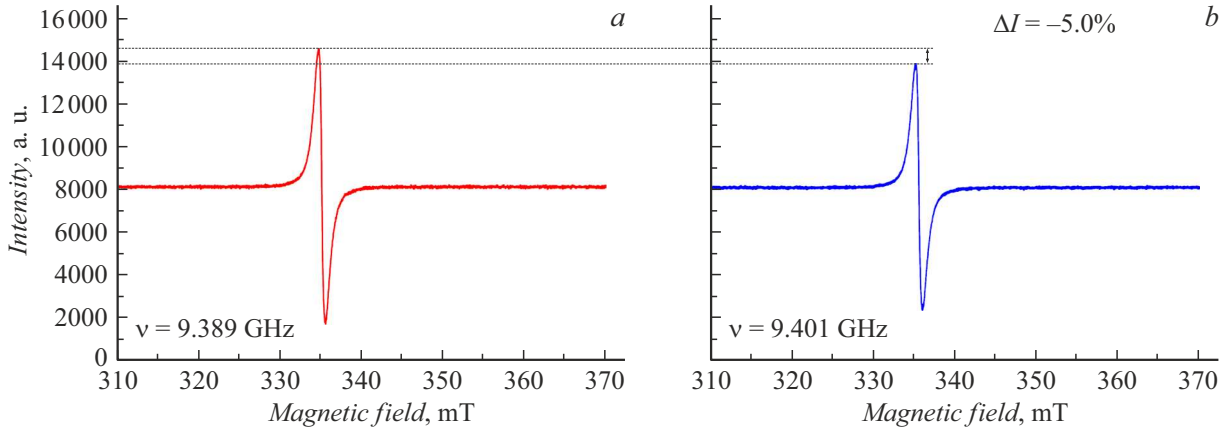

Figure 4. ESR spectra of initial DND (*a*) and CTAB-modified DND (*b*).

containing groups. Thus, for example, the presence of a band in the 1283 cm^{-1} region in the spectrum is due to bending vibrations of the O−H fragment, which is part of the carboxyl groups.

An intense line at 1795 cm^{-1} corresponds to the C=O bond vibrations. A shift from the literary value typical for carboxylic acids ($\sim 1725 - 1700\,cm^{-1}$ [47]), indicates a high degree of oxidation of the surface of DND and the fact that in addition to the functional groups of carboxylic acids, aldehydes and ketones, ester (in particular, lactone) and anhydride groups are also localized on the surface [47]. It is important to note that the IR spectra were recorded for dry DND powder, dispersion of such sample in water results in hydrolysis of anhydrides and esters with the formation of carboxylic acids and alcohols [25].

An intense band at 1409cm^{-1} in the spectrum should be attributed to valence vibrations of the C−O bond, and at 1627 cm^{-1}, deformation vibrations of water adsorbed on the surface of DND or surface −OH groups are observed. This spectrum is also characterized by the presence of a wide band of high intensity in the 3500 cm^{-1} region, corresponding to stretching vibrations of intra- and intermolecular hydrogen bonds of hydroxyl groups. The presence of adsorbed water absorption bands in the spectrum complicates significantly the unambiguous interpretation of the nature of absorption peaks of hydroxyl (−OH)-groups, however, it is well known that DND also contains −OH surface groups [39]. A line at 1119 cm^{-1} corresponds to asymmetric stretching of the C−O−C group as part of the C−C(=O)−O fragment that belongs to lactones or esters. Based on the results of electron microprobe, it is possible to assume the presence of valence vibrations of the C−Cl bond detected at 668 cm^{-1}.

Detailed interpretation of bands in the DND IR spectrum is given in Table 2. The following notations were used: ν — stretching, δ — bending vibrations.

Dissociation of ionogenic (carboxyl and hydroxyl) functional DND surface groups causes the negative particle charge in hydrosols. According to the ELS data, elec-

Table 2. Interpretation of IR spectrum of initial DND

№	Wavenumber, cm^{-1}	Type of vibration and assignment	Source
1	3400	ν(OH) Intramolecular and intermolecular hydrogen bonds	[48-53]
2	1795	ν(C=O)	[48-53]
3	1627	δ(H–O–H)	[48-53]
4	1409	ν(C–O)	[49-51]
5	1283	δ(C–O–H)	[49,50]
6	1119	ν_{as}(C–O–C)	[49,50]
7	668	ν(C–Cl)	[49,51]

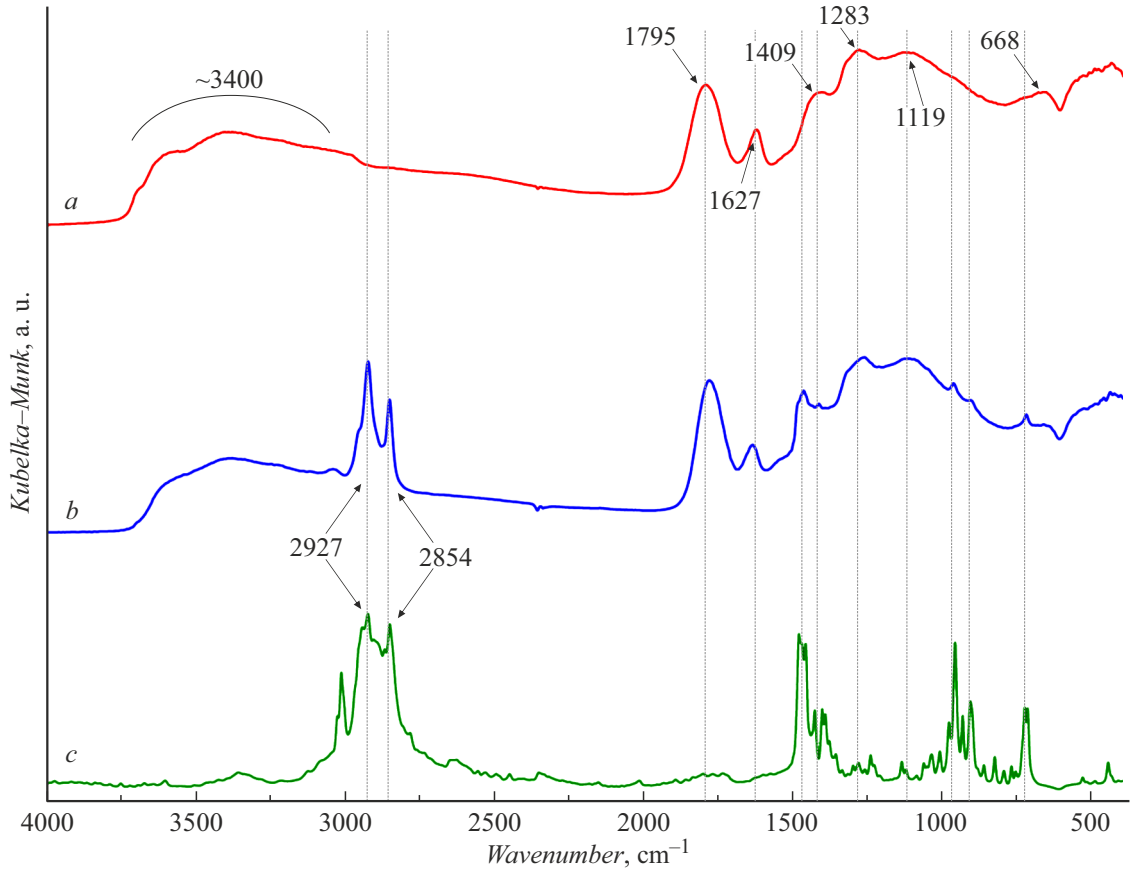

Figure 5. IR spectra of initial DND (a), DND−CTAB (b), CTAB (c).

trokinetic potential of the initial DND sample in hydrosol is (-58.06 ± 2.66) mV.

Experimental IR spectrum of CTAB (Figure 5, c) agrees with the spectra reported in [54,55] and is characterized by intense bands at $3000-2800\,cm^{-1}$ corresponding to various stretching of the CH_2 and CH_3 groups. In the area below $1500\,cm^{-1}$ and low-frequency spectrum region known as the „fingerprint“ region ($1300-650\,cm^{-1}$), numerous bending vibration bands of the same groups and N−C bonds are observed [48].

3.2. Investigation of DND surface modification by CTAB surfactant

IR spectrum of the CTAB-modified nanodiamond sample (Figure 5, b) retains most bands typical of the initial DND, moreover high-intensity bands occur at 2855 and $2927\,cm^{-1}$, that are clearly indicative of C–H stretching in methyl and hexadecyl groups of the cetyltrimethylammonium bromide chain. The absence of absorption bands of cetyltrimethylammonium bromide in the UV-Vis spectrum

of supernatant and the appearance of bands typical of CTAB in the DND IR spectrum are indicative of the fact that surfactant molecules have been fixed on the surface of DND particles.

According to the electron microprobe analysis (Table 1), relative content of elements in the sample didn't change after DND surface modification. However, it is important to note that there are no signals of the bromine atom concentration of which in the inoculated amount of surfactant is sufficient for detection by the EMP. This fact together with the IR spectroscopy data prove that there is a surfactant on the DND surface in the cation form. The absence of nitrogen atom signals is due to its obviously small mass fraction in the sample, coupled with the limitation of the method, which consists in its significantly lower sensitivity to the content of light elements [56].

The ELS data demonstrates change of the electrokinetic potential in water from (-58.06 ± 2.66) mV for the initial DND to (-30.83 ± 0.50) mV for the modified DND, which, taking into account the almost complete removal of non-interacting CTAB amounts, indicates a modification of the surface.

The DLS study (Figure 2, *b*) shows that the DND particle sizes increase in hydrosols after modification. It can be seen that that the mean particle size recorded by this method has changed from 4 to ~ 120 nm, and the distribution is unimodal — there are particle sizes of only hundreds of nm and there are no larger and, interestingly, smaller particles.

Our quantum chemical calculations in Gaussian-09 software [57] at the B3LYP/6-311G (d, p) theory level show that the hydrocarbon tail length of CTAB is ~ 2 nm, i.e. when CTAB is inoculated on the DND surface, diameter of one particle can increase to ~ 8 nm maximum, which is much lower than the experimental size. Thus, DND particles and CTAB in aqueous medium are bonded in a kind of agglomerate. In addition, it is known from [58,59] that, as the concentration increases, CTAB is prone to formation of double layers on nanoparticle surfaces or micelles around nanoparticles. Therefore, this experimental fact must be investigated separately, for example, by small-angle X-ray and neutron scattering.

In general, reduction of the aggregative stability of modified DND particles in water suggests higher hydrophobicity of their surface.

Within the method accuracy, the ESR spectra of the initial and modified DND samples (Figure 4) are the same: difference in intensity (5.0%) is smaller than the relative measurement error of unpaired electron concentration by the ESR method that is 15–20% [60]. The modified DND sample also has $g = 2.0019$. Thus, the DND–CTAB bond is not formed due to the unpaired electrons of the diamond nanoparticle.

All the aforesaid confirms DND surface modification by cetyltrimethylammonium bromide. The suggested mechanism of DND–CTAB bond formation is illustrated in Figure 6. Note that in [61] it is supposed that DND and CTAB are bonded through hydrogen bonds via bridging water molecules, but no firm evidence of the proposed mechanism is provided. We believe that the nature of the DND and CTAB bond must be studied separately.

3.3. Stability assessment of dimethyl sulfoxide-based sols

The absorption spectra (Fig. 7, *b*, *c*, line *2*) demonstrate the invariance over time of the absorption value of the DND–CTAB sol in DMSO, while the absorption intensity of the sol of the initial DND in DMSO (Fig. 7, *a*, *c*, curve *1*) decreases exponentially over all wavelengths, which is a direct proof of the stability of sols DND–CTAB in DMSO and its absence in the case of sol of the initial DND in DMSO. The wavelength range of less than 400 nm is not informative, since the observed intensity exceeds the photometric range of the device.

ELS measurements show that the value of the electrokinetic potential for the initial DND particles in sol immediately after preparation is (-31.8 ± 1.6) mV. Moreover, according to the data obtained by the DLS immediately after completion of sol synthesis, the size distribution maximum of the initial DND particles in DMSO (Figure 8, *a*) is ~ 4 nm.

It is obvious that instability of the DND sol with oxidized surface in DMSO is associated with insufficient absolute value of electrokinetic potential for effective electrostatic repulsion of particles. It is clear that, other factors being equal, the absolute threshold value of the ξ-potential increases with the transition to solvents of lower polarity.

Previously, the instability of DND sols with an oxidized surface in DMSO was associated with the acidity of the surface of carboxylated DND particles. According to the authors [33], the presence of a large number of carboxyl groups on the surface of DND causes the decomposition of DMSO molecules, which later apparently leads to the aggregation of diamond nanoparticles.

However, we believe that failure to achieve stable sols of carboxylated DND particles in DMSO is explained mainly by the fact that polar aprotic solvents solvate anions poorly. As mentioned above, this is associated with steric difficulties that occur when the anion approaches the partially positive charge area of the DMSO molecule. At the same time, the experimentally shown negative sign of the electrokinetic potential suggests the presence of oxidized DND particles in DMSO in the anionic form, which is likely caused by the dissociation of carboxyl groups of the DND surface. This is why carboxylated diamond nanoparticles produced by detonation synthesis not subjected to any surface modification form instable colloidal solutions in dimethyl sulfoxide.

According to the DLS data obtained immediately upon completion of the sol synthesis, size distribution maximum of the DND–CTAB particles in DMSO (Figure 8) is 27 nm. ELS measurements show that the electrokinetic potential of the DND–CTAB particles in DMSO immediately after

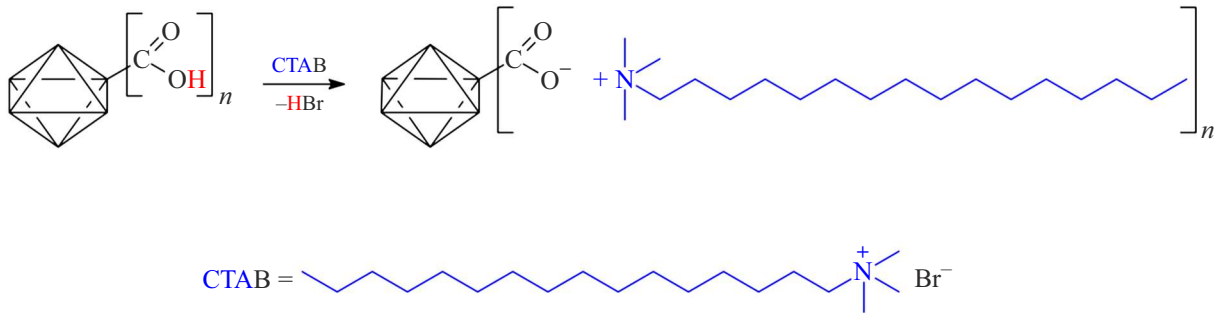

Figure 6. Anticipated scheme of interaction between DND and CTAB.

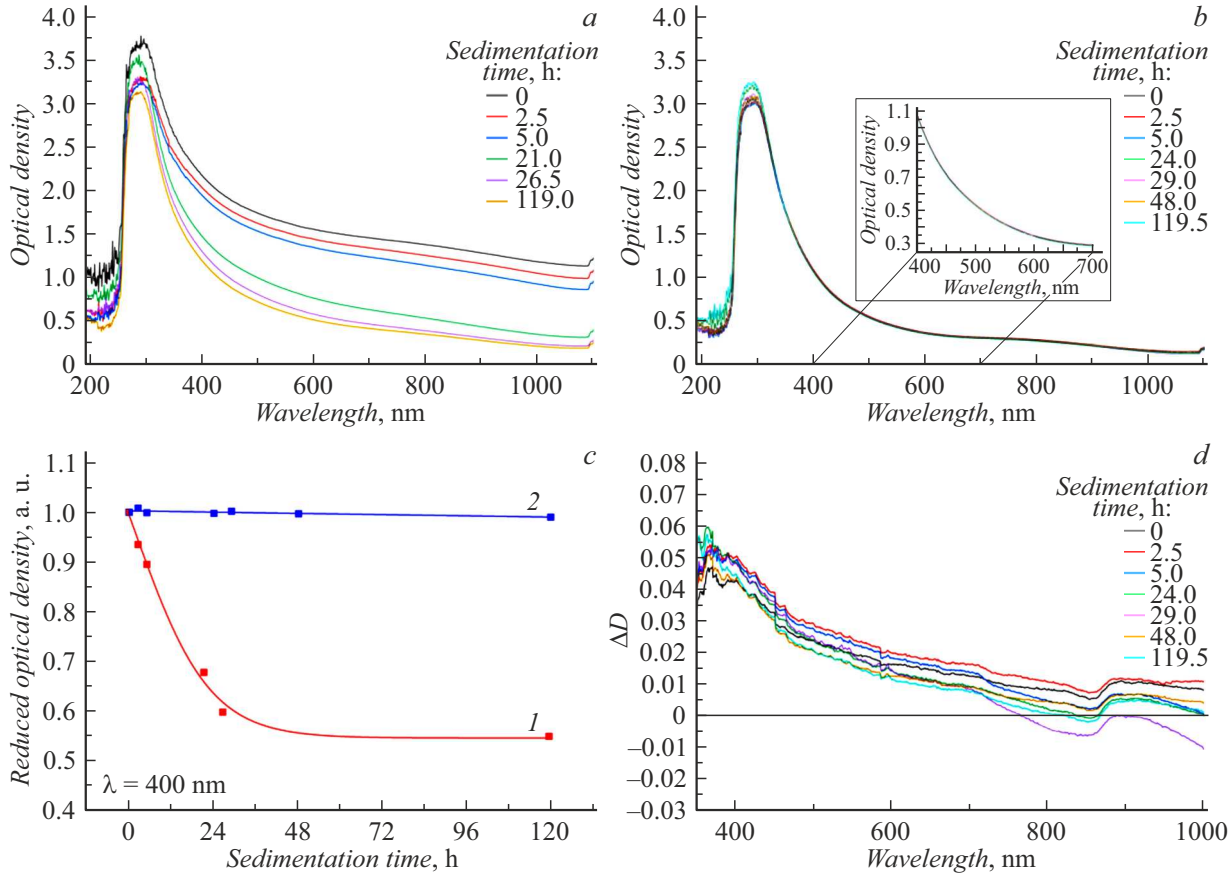

Figure 7. Time evolution of the absorption spectra of the initial (*a*) and CTAB-modified (*b*) DND in DMSO; change of reduced (normalized to the first measurement) absorbance of the initial (*c*, curve *1*) and CTAB-modified (*c*, line *2*) DND in DMSO with time at 400 nm; evolution of difference absorption spectra of CTAB-modified DND in DMSO (*d*).

sol preparation is (-14.0 ± 1.0) mV, which is lower in the absolute value than for the non-modified sample sol.

It is known that a higher absolute value of the electrokinetic potential causes higher stability of colloidal solution particles due to higher electrostatic repulsion of particles [62]. Nevertheless, the modified DND sample shows colloidal stability in DMSO in time compared with the initial sample. This has been already shown by the UV-Vis spectroscopy. Furthermore, dark greenish yellow jellylike sediment was observed in the initial DND sol after settlement during a month, while no sediment was observed in the modified nanodiamond solution in DMSO. Sedimentation stability of the DND–CTAB sol in DMSO is also confirmed by higher intensity of the Tyndall effect for the modified DND sol when laser beam is transmitted through solutions. Thus, electrokinetic potential in this case cannot serve as a sol stability criterion because the sol stabilization mechanism differs from the electrostatic one (typical of hydrosols) for which the ξ-potential is responsible.

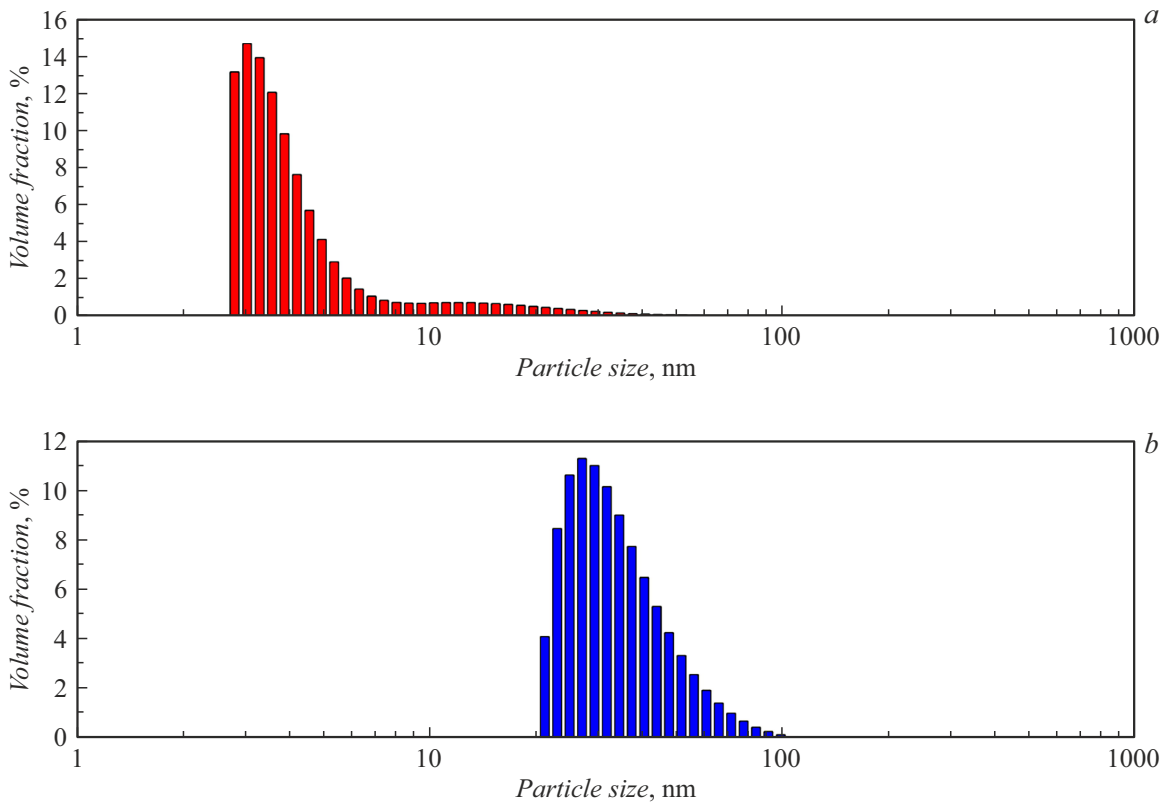

Figure 8. Size distribution of initial DND (*a*) and CTAB-modified DND particles (*b*) in DMSO-based sol immediately after preparation.

Analysis of difference spectra (Figure 7, *d*) shows the absence of soft clusters for the DND−CTAB system in DMSO similar to those detected in [63]. As can be seen from the difference spectra, scattering intensity tends to zero, i.e. the DND−CTAB particles are not combined into extended loose formations and their stability is not associated with formation of an extended pseudo polymer network that is stable to the Brownian movement.

The larger size of the DND−CTAB particles in DMSO together with small electrostatic repulsion are indicative of the steric sol stability mechanism.

Note that as a result of modification of the surface of diamond nanoparticles by CTAB molecules not all ionogenic (carboxyl and hydroxyl) functional DND groups were bonded to the surfactant. Therefore the produced stable sols may be considered as a promising material that can be used for future modification of the DND surface in the DMSO medium. The proposed approach will provide stable colloidal solutions of diamond nanoparticles modified by ions of various metals [6], proteins [64], etc., carrying out this process in two stages. New synthetic opportunities are offered to conduct reactions based on the S_N2 mechanism which rates in the dimethyl sulfoxide medium are expected to be higher than, for example, in aqueous medium. In particular, it opens up the possibility of obtaining ethers by the Williamson reaction and esters by interaction between the surface functional groups of carboxylic acid salts and alkyl halides or diazomethane, etc. [25,26]

Conclusion

The work proposes an explanation for the instability of oxidized DND particles sols in dimethyl sulfoxide due to weak solvation of anions by dimethyl sulfoxide molecules.

It is shown that modification of the surface of diamond nanoparticles produced by detonation synthesis of detonation synthesis surfaces with negative electrokinetic potential by a cationic surfactant — cetyltrimethylammonium bromide — makes it possible to produce stable sols with a mean particle size of 27 nm in an organic solvent — dimethyl sulfoxide. Using the data obtained by dynamic and electrophoretic light scattering, a steric mechanism of DND–CTAB sols stability in DMSO is proposed.

As only a part of ionogenic groups on the DND surface undergoes reaction during CTAB modification, the proposed method of DND sol stabilization in DMSO may be used for future modification of the surface of diamond nanoparticles by other chemical reagents.

Acknowledgments

Studies by the electron microprobe and X-ray powder diffraction were performed using the equipment provided by the Engineering Center of St. Petersburg State Institute of Technology (Technical University). Quantum chemical calculations were conducted using the High-Performance

Computing Cluste of St. Petersburg State Institute of Technology (Technical University).

Funding

The study was performed under state assignment of Ioffe Institute FFUG-2024-0019.

Conflict of interest

The authors declare no conflict of interest.

References

[1] A.Ya. Vul', O.A. Shenderova (red.). *Detonatsyonnye nanoalmazy. Tekhnologiya, struktura, svoistva i primeneniya* (Izdvo FTI im. A.F. Ioffe, SPb, 2016) (in Russian).
[2] V.Yu. Dolmatov, A.N. Ozerin, I.I. Kulakova, O.O. Bochechka, N.M. Lapchuk, V. Myllymäki, A. Vehanen. Russ. Chem. Rev., **89** (12), 1428 (2020). DOI: 10.1070/RCR4924
[3] L. Basso, M. Cazzanelli, M. Orlandi, A. Miotello. Appl. Sci., **10** (12), 4094 (2020). DOI: 10.3390/app10124094
[4] P. Karami, S. Salkhi Khasraghi, M. Hashemi, S. Rabiei, A. Shojaei. Adv. Colloid Interface Sci., **269**, 122 (2019). DOI: 10.1016/j.cis.2019.04.006
[5] D. Terada, T.F. Segawa, A.I. Shames, S. Onoda, T. Ohshima, E. Ōsawa, R. Igarashi, M. Shirakawa. ACS Nano, **13** (6), 6461 (2019). DOI: 10.1021/acsnano.8b09383
[6] A.S. Chizhikova, E.B. Yudina, A.M. Panich, M. Salti, Yu.V. Kulvelis, A.I. Shames, O. Prager, E. Swissa, A.E. Aleksinski, A.Ya. Vul. ZhTF, **94** (9), 1474 (2024). (in Russian) DOI: 10.61011/JTF.2024.09.58667.70-24
[7] J. Lazovic, E. Goering, A. Wild, P. Schützendübe, A. Shiva, J. Löffler, G. Winter, M. Sitti. Adv. Mater., **36** (11), 2310109 (2024). DOI: 10.1002/adma.202310109
[8] A.V. Shvidchenko, E.D. Eidelman, A.Ya. Vul', N.M. Kuznetsov, D.Yu. Stolyarova, S.I. Belousov, S.N. Chvalun. Adv. Colloid Interface Sci., **268**, 64 (2019). DOI: 10.1016/j.cis.2019.03.008
[9] A. Krüger, F. Kataoka, M. Ozawa, T. Fujino, Y. Suzuki, A.E. Aleksenskii, A.Ya. Vul', E. Ōsawa. Carbon, **43** (8), 1722 (2005). DOI: 10.1016/j.carbon.2005.02.020
[10] O.A. Williams, J. Hees, C. Dieker, W. Jäger, L. Kirste, C.E. Nebel. ACS Nano, **4** (8), 4824 (2010). DOI: 10.1021/nn100748k
[11] A.E. Aleksenskiy, E.D. Eydelman, A.Ya. Vul'. Nanosci. Nanotechnol. Lett., **3** (1), 68 (2011). DOI: 10.1166/nnl.2011.1122
[12] N. Nunn, M. Torelli, G. McGuire, O. Shenderova. Current Opinion in Solid State and Mater. Sci., **21** (1), 1 (2017). DOI: 10.1016/j.cossms.2016.06.008
[13] Y.-J. Zhai, Z.-C. Wang, W. Huang, J.-J. Huang, Y.-Y. Wang, Y.-Q. Zhao. Mater. Sci. Engineer.: A, **528** (24), 7295 (2011). DOI: 10.1016/j.msea.2011.06.053
[14] I. Neitzel, V. Mochalin, I. Knoke, G.R. Palmese, Y. Gogotsi. Compos. Sci. Technol., **71** (5), 710 (2011). DOI: 10.1016/j.compscitech.2011.01.016
[15] E.V. Sivtsov, A.V. Kalinin, A.I. Gostev, A.V. Smirnov, L.B. Agibalova, F.A. Shumilov. Vysokomolek. soed. B, **62**, 6 (465) (in Russian) DOI: 10.31857/S2308113920050137
[16] S. Banerjee, R. Sharma, K.K. Kar. In: *Composite Materials* ed. by K.K. Kar (Berlin, Heidelberg, Springer Berlin Heidelberg, 2017), p. 251–280. DOI: 10.1007/978-3-662-49514-8_8
[17] Z. Chen, Y. Liu, J. Luo. Colloids and Surfaces A: Physicochemical and Engineering Aspects, **489**, 400 (2016). DOI: 10.1016/j.colsurfa.2015.10.062
[18] G. Żyła, J.P. Vallejo, J. Fal, L. Lugo. Intern. J. Heat Mass Transfer, **121**, 1201 (2018). DOI: 10.1016/j.ijheatmasstransfer.2018.01.073
[19] M. Nishikawa, M. Liu, T. Yoshikawa, H. Takeuchi, N. Matsuno, N. Komatsu. Carbon, **205**, 463 (2023). DOI: 10.1016/j.carbon.2023.01.025
[20] N. Nunn, O. Shenderova. Phys. Status Solidi A, **213** (8), 2138 (2016). DOI: 10.1002/pssa.201600224
[21] T. Dolenko, S. Burikov, K. Laptinskiy, J.M. Rosenholm, O. Shenderova, I. Vlasov. Phys. Status Solidi A, **212** (11), 2512 (2015). DOI: 10.1002/pssa.201532203
[22] V.N. Mochalin, Y. Gogotsi. J. Am. Chem. Soc., **131** (13), 4594 (2009). DOI: 10.1021/ja9004514
[23] C.-C. Li, C.-L. Huang. Colloids Surf. Physicochem. Eng. Asp., **353** (1), 52 (2010). DOI: 10.1016/j.colsurfa.2009.10.019
[24] Yu.N. Kukushkin Sorosovskiy obrazovatel'nyy zhurnal, **9** (54), (1997) (in Russian).
[25] J. Clayden, N. Greeves, S. Warren. *Organic chemistry* (Oxford university press, Oxford, 2012)
[26] D.R. Klein. *Organic chemistry* (Wiley, Hoboken, NJ., 2021)
[27] Z. Tashrifi, M.M. Khanaposhtani, B. Larijani, M. Mahdavi. Adv. Synthesis Catalysis, **362** (1), 65 (2020). DOI: 10.1002/adsc.201901021
[28] M.V. Polynski, M.D. Sapova, V.P. Ananikov. Chem. Sci., **11** (48), 13102 (2020). DOI: 10.1039/D0SC04752J
[29] D.A. Tebbe, C. Gruender, L. Dlugosch, K. Lõhmus, S. Rolfes, M. Könneke, Y. Chen, B. Engelen, H. Schäfer. The ISME J., **17** (12), 2340 (2023). DOI: 10.1038/s41396-023-01539-1
[30] J. Capriotti, K. Capriotti. Int. Med. Case Rep. J., **8**, 231 (2015). DOI: 10.2147/IMCRJ.S90775
[31] D. Ho. *Nanodiamonds: applications in biology and nanoscale medicine* (Springer, NY., 2010)
[32] A.C. Williams, B.W. Barry. Adv. Drug. Deliv. Rev., **56** (5), 603 (2004). DOI: 10.1016/j.addr.2003.10.025
[33] O. Shenderova, S. Hens, G. McGuire. Diam. Relat. Mater., **19** (2–3), 260 (2010). DOI: 10.1016/j.diamond.2009.10.008
[34] N.O. Mchedlov-Petrossyan, N.N. Kriklya, A.N. Laguta, E. Ōsawa. Liquids, **2** (3), 196 (2022). DOI: 10.3390/liquids2030013
[35] A.E. Aleksenskii, A.S. Chizhikova, V.I. Kuular, A.V. Shvidchenko, E.Yu. Stovpiaga, A.D. Trofimuk, B.B. Tudupova, A.N. Zhukov. Diam. Relat. Mater., **142**, 110733 (2024). DOI: 10.1016/j.diamond.2023.110733
[36] L. Fang, H. Lei, Y. Cao, J. Wang, Y. Yang, W. Wang. Diam. Relat. Mater., **128**, 109236 (2022). DOI: 10.1016/j.diamond.2022.109236
[37] Yu.Ya. Fialkov, A.N. Zhitomirsky, Yu.A. Tarasenko. *Fizicheskaya khimiya nevodnykh rastvorov* (Khimiya, L., 1973) (in Russian)
[38] Yu.Ya. Fialkov. *Rastvoritel kak sredstvo upravleniya khimicheskim protsessom* (Khimiya, L., 1990)
[39] A.V. Shvidchenko. *Sruktura i svoistva poverkhtosti svobodnykh tchastits detonatsionnogo nanoalmaza* (kand. diss., FTI im. A.F. Ioffe RAN, SPb., 2018) (in Russian)

[40] S. Haghighatafshar, E. Hallinger, D. Espinoza, B. Al-Rudainy. Water Pract. Technol., **19** (5), 1810 (2024). DOI: 10.2166/wpt.2024.040
[41] G. Cunningham, M. Lotya, C.S. Cucinotta, S. Sanvito, S.D. Bergin, R. Menzel, M.S.P. Shaffer, J.N. Coleman. ACS Nano, **6** (4), 3468 (2012). DOI: 10.1021/nn300503e
[42] K. Maleski, V.N. Mochalin, Y. Gogotsi. Chem. Mater., **29** (4), 1632 (2017). DOI: 10.1021/acs.chemmater.6b04830
[43] P.N. Nesterenko, D. Mitev, B. Paull. In: *Nanodiamonds. Advanced Material Analysis, Properties and Applications*, ed. by J.-C. Arnault (Amsterdam, Elsevier, 2017), p. 109–130.
[44] M. Mermoux, S. Chang, H.A. Girard, J.-C. Arnault. Diam. Relat. Mater., **87**, 248 (2018). DOI: 10.1016/j.diamond.2018.06.001
[45] A. Krueger. *Carbon materials and nanotechnology* (Wiley-VCH, Weinheim, 2010)
[46] A.I. Shames, A.M. Panich, W. Kempiński, A.E. Alexenskii, M.V. Baidakova, A.T. Dideikin, V.Yu. Osipov, V.I. Siklitski, E. Osawa, M. Ozawa, A.Ya. Vul'. J. Phys. Chem. Sol., **63** (11), 1993 (2002). DOI: 10.1016/S0022-3697(02)00185-3
[47] V.F. Traven. *Organicheskaya khimiya* (Laboratoriya znaniy, M., 2021) (in Russian)
[48] K. Nakanisi. *Infrakrasnye spektry i stroenie organicheskikh soedineniy*, pod red. A.A. Maltseva; per. N.B. Kupletskaya, L.M. Epstein (Mir, M., 1965) (in Russian)
[49] B.N. Tarasevich. *IK spektry osnovnykh klassov organicheskikh soedinenii. Spravochnye materialy* (MGU im M.V. Lomonosova, khimichesky facultet, kafedra organicheskoi khimii, M., 2012) (in Russian).
[50] A.N. Zhukov, A.V. Shvidchenko, E.B. Yudina. Colloid J., **82** (4), 369 (2020). DOI: 10.1134/S1061933X20040171
[51] T. Petit, L. Puskar. Diam. Relat. Mater., **89**, 52 (2018). DOI: 10.1016/j.diamond.2018.08.005
[52] V.Yu. Dolmatov, A.N. Ozerin, A.P. Voznyakovsky, A.A. Voznyakovsky, N.M. Lapchuk, A.I. Shames, A.M. Panich. Izvestiya SPbGTI(TU), **66** (92), 31 (2023) (in Russian). DOI: 10.36807/1998-9849-2023-66-92-31-34
[53] M.S. Shestakov, S.P. Vul', A.T. Dideikin, T.V. Larionova, A.V. Shvidchenko, E.B. Yudina, V.V. Shnitov. J. Phys. Conf. Ser., **1400** (5), 055044 (2019). DOI: 10.1088/1742-6596/1400/5/055044
[54] G. Su, C. Yang, J.-J. Zhu. Langmuir, **31** (2), 817 (2015). DOI: 10.1021/la504041f
[55] F. Ai, G. Zhao, W. Lv, J. Lin. Mater. Res. Express, **7** (8), 085008 (2020). DOI: 10.1088/2053-1591/abad15
[56] M.M. Krishtal, I.C. Yasnikov, V.I. Polunin, A.M. Filatov, A.G. Ulyanenkov. *Skaniruyushchaya elekronnaya mikroskopiya i rentgenospekralnyi mikroanaliz v primerakh prakticheskogo primeneniya* (Tekhnosfera, M., 2009) (in Russian)
[57] M.J. Frisch, G.W. Trucks, H.B. Schlegel, G.E. Scuseria, M.A. Robb, J.R. Cheeseman, G. Scalmani, V. Barone, B. Mennucci, G.A. Petersson, H. Nakatsuji, M. Caricato, X. Li, H.P. Hratchian, A.F. Izmaylov, J. Bloino, G. Zheng, J.L. Sonnenberg, M. Hada, M. Ehara, K. Toyota, R. Fukuda, J. Hasegawa, M. Ishida, T. Nakajima, Y. Honda, O. Kitao, H. Nakai, T. Vreven, J.A. Montgomery, Jr., J.E. Peralta, F. Ogliaro, M. Bearpark, J.J. Heyd, E. Brothers, K.N. Kudin, V.N. Staroverov, T. Keith, R. Kobayashi, J. Normand, K. Raghavachari, A. Rendell, J. C. Burant, S.S. Iyengar, J. Tomasi, M. Cossi, N. Rega, J.M. Millam, M. Klene, J.E. Knox, J.B. Cross, V. Bakken, C. Adamo, J. Jaramillo, R. Gomperts, R.E. Stratmann, O. Yazyev, A.J. Austin, R. Cammi, C. Pomelli, J.W. Ochterski, R.L. Martin, K. Morokuma, V.G. Zakrzewski, G.A. Voth, P. Salvador, J.J. Dannenberg, S. Dapprich, A.D. Daniels, O. Farkas, J.B. Foresman, J.V. Ortiz, J. Cioslowski, D.J. Fox, Gaussian, Inc., Wallingford CT, 2013.
[58] S. Skoglund, E. Blomberg, I.O. Wallinder, I. Grillo, J.S. Pedersen, L.M. Bergström. Phys. Chem. Chem. Phys., **19** (41), 28037 (2017). DOI: 10.1039/C7CP04662F
[59] R. Li, Z. Wang, X. Gu, C. Chen, Y. Zhang, D. Hu. ACS Omega, **5** (10), 4943 (2020).
[60] V.A. Rabinovich, Z.Ya. Khavin, *Kratkiy khimichesliy spravochnik* (Khimiya, L.,1978) (in Russian)
[61] G.A. Badun, M.G. Chernysheva, A.V. Gus'kov, A.V. Sinolits, A.G. Popov, A.V. Egorov, T.B. Egorova, I.I. Kulakova, G.V. Lisichkin. Fullerenes, Nanotubes and Carbon Nanostructures, **28** (5), 361 (2020). DOI: 10.1080/1536383X.2019.1685982.
[62] D.J. Shaw. *Introduction to colloid and surface chemistry* (Butterworth-Heinemann, Oxford, 1992)
[63] O.V. Tomchuk, M.V. Avdeev, A.T. Dideikin, A.Ya. Vul', A.E. Aleksenskii, D.A. Kirilenko, O.I. Ivankov, D.V. Soloviov, A.I. Kuklin, V.M. Garamus, Yu.V. Kulvelis, V.L. Aksenov, L.A. Bulavin. Diam. Relat. Mater., **103**, 107670 (2020). DOI: 10.1016/j.diamond.2019.107670
[64] H.-D. Wang, Q. Yang, C.H. Niu, I. Badea. Diam. Relat. Mater., **20** (8), 1193 (2011). DOI: 10.1016/j.diamond.2011.06.015

Translated by E.Ilinskaya